Process Biochemistry 110 (2021) 263–274

Contents lists available at ScienceDirect

Process Biochemistry

journal homepage: www.elsevier.com/locate/procbio

Non-enzymatic properties *of Proteus mirabilis* urease subunits

Valquiria Broll [a,1], Ana Paula A. Perin [a,1], Fernanda C. Lopes [a], Anne Helene S. Martinelli [b], Natalia R. Moyetta [a,c,2], Leonardo L. Fruttero [a,c,d,2], Matheus V.C. Grahl [c,d], Augusto F. Uberti [c,d], Diogo R. Demartini [a], Rodrigo Ligabue-Braun [a,3,*], Celia R. Carlini [a,c,d,*]

[a] Center of Biotechnology, Graduate Program in Cellular and Molecular Biology, Universidade Federal do Rio Grande do Sul (UFRGS), Porto Alegre, RS, CEP 91501-970, Brazil
[b] Department of Biophysics & Department of Molecular Biology and Biotechnology, Biosciences Institute, UFRGS, Porto Alegre, RS, 91501-970, Brazil
[c] Brain Institute (BRAINS) – InsCer and School of Medicine, Pontifícia Universidade Católica do Rio Grande do Sul (PUCRS), Porto Alegre, RS, CEP 90610-000, Brazil
[d] Graduate Program in Medicine and Health Sciences, Pontifícia Universidade Católica do Rio Grande do Sul (PUCRS), Porto Alegre, RS, CEP 90610-000, Brazil

ARTICLE INFO

Keywords:
Urease
Proteus mirabilis
Uropathogen
PmUreβ
Candida albicans
Moonlighting proteins

ABSTRACT

Ureases are moonlighting proteins displaying non-catalytic properties, including platelet activation, antifungal and entomotoxic effects. The structure-activity mapping of these properties is poorly developed. *Proteus mirabilis* urease (PMU) consists of three subunits, PmUreα, PmUreβ and PmUreγ, in an $(\alpha\beta\gamma)_3$ organization. In order to study the structure-activity relationships of PMU we obtained the recombinant subunits of this urease and evaluated their biological activities. The holo-urease promoted platelet aggregation, and toxicity in fungal and insect models. Similar to Jaburetox, a plant urease-derived polypeptide, PmUreβ showed the highest toxicity against yeasts and insects, and activated human platelets. PmUreγ and PmUreα presented insecticidal action upon injection. In addition, only PmUreγ and PmUreβ promote hemocytes aggregation. Bioinformatics analyses revealed gene/segment duplication and evolutionary divergence among ureases. Our findings show that PmUreβ (and probably its counterparts in other ureases) carries most of the non-enzymatic activities of these proteins.

1. Introduction

Ureases (EC 3.5.1.5) are nickel-dependent enzymes that catalyze the hydrolysis of urea into ammonia and carbamate, which spontaneously decompose into carbon dioxide and a second molecule of ammonia [1–3]. Ureases are well conserved proteins although differing in their quaternary structures. While plant and fungal ureases are hexamers of a single chain subunit, bacterial ureases can be trimers, hexamers, or dodecamers, whose "monomers" are composed by two or three hetero-subunits that co-align with the single chained ureases [4–7].

In the last two decades, ureases have been characterized as moonlighting proteins that display many other biological properties unrelated to catalysis. The ammonia-independent toxicity of ureases was initially described for Canatoxin, an isoform of the jack bean (*Canavalia ensiformis*) urease, which causes convulsions preceding death of mice and rats. Canatoxin, and also the classic jack bean urease (JBU), have insecticidal and fungitoxic properties. Most of the non-enzymatic activities of Canatoxin and JBU were also observed for ureases from other plants (soybean, cotton) and for the bacterial enzymes of *Helicobacter pylori* and *Sporosarcina* (*Bacillus*) *pasteurii* [1,4].

Structures *versus* activity studies on the moonlighting properties of ureases are scarce. An internal sequence encompassing 91 amino acids of *C. ensiformis* ureases was found to carry their insecticidal activity. Recombinant polypeptides with equivalent sequences were built and named Jaburetox, with 93 amino acids (~11 kDa), derived from JBURE-II, an isoform of JBU, [8,9], and Soyuretox, homologous to Jaburetox, but derived from the sequence of the ubiquitous isoform of the soybean urease [10]. In addition to entomotoxicity, Jaburetox and Soyuretox are

* Corresponding authors at: Center of Biotechnology, Graduate Program in Cellular and Molecular Biology, Universidade Federal do Rio Grande do Sul (UFRGS), Porto Alegre, RS, CEP 91501-970, Brazil.
E-mail addresses: rodrigolb@ufcspa.edu.br (R. Ligabue-Braun), celia.carlini@pucrs.br (C.R. Carlini).
[1] These authors contributed equally to this work.
[2] Present address: Departamento de Bioquímica Clínica, Facultad de Ciencias Químicas, Universidad Nacional de Córdoba, Córdoba, Argentina. Centro de Investigaciones en Bioquímica Clínica e Inmunología (CIBICI), Consejo Nacional de Investigaciones Científicas y Técnicas (CONICET), Córdoba, Argentina;
[3] Present address: Department of Pharmacosciences, Universidade Federal de Ciências da Saúde de Porto Alegre (UFCSPA), Porto Alegre, RS, Brazil.

https://doi.org/10.1016/j.procbio.2021.08.023
Received 30 March 2021; Received in revised form 6 August 2021; Accepted 23 August 2021
Available online 25 August 2021

also toxic to filamentous fungi and yeasts, but do not activate platelets, nor display lethality towards rodents, also Soyuretox is not toxic to zebrafish embryos [9,10]. Altogether these data pointed to the existence of more than one biologically active domain in ureases [8–11].

H. pylori urease (HPU), a crucial virulence factor of this bacterium, which causes gastritis, ulcers and stomach cancer [12] consists of two chains, HpUreA (27 kDa), representing a fusion of the γ and β domain of other bacterial enzymes, and HpUreB (61 kDa), which contains the active site [1]. HpUreB was shown to interact with CD74 on T cells and with Th17 lymphocytes [13]. HpUreA was found in the nucleus of gastric epithelial cells [14]. Although both subunits of HPU were able to bind to platelets, only HpUreB displayed platelet-aggregating properties [15].

Proteus mirabilis is a gastrointestinal Gram-negative bacillus and an opportunistic uropathogen, whose infection typically leads to formation of bladder and kidney stones along with catheter-associated urinary infections [16,17]. *Proteus mirabilis* produces a urea-inducible urease (PMU) well recognized as a virulence factor [16,18]. Other virulence factors, such as fimbriae and adhesins, act cooperatively with PMU in the pathogenesis of urinary infection [16,19]. The enzyme activity of PMU enables the pathogen to hydrolyze urea into carbon dioxide and ammonia, thus providing nitrogen for bacterial survival. Subsequently the generated ammonia alkalinizes the urine, resulting in precipitation of urinary salts and formation of urinary stones that are colonized by bacteria [20].

P. mirabilis urease has three subunits, PmUreA or PmUreγ (11.0 kDa), PmUreB or PmUreβ (12.2 kDa) and PmUreC or PmUreα (66.0 kDa), organized in an $(\alpha\beta\gamma)_3$ oligomer [21,22]. In this work, we have studied PMU and its recombinant subunits separately, aiming to determine if PMU is also a multifunctional protein and to get structural insights of its biological activities.

2. Materials and methods

2.1. Plasmid construction and bacterial strain

Escherichia coli HB101 carrying a pMID 1010 plasmid was a kind gift from Dr. Harry T. Mobley (Department of Microbiology and Immunology, University of Michigan Medical School, Ann Arbor, MI, USA). This plasmid contains the complete operon for PMU formed by eight genes *in tandem*: three structural genes (*ure*A, *ure*B and *ure*C) and five genes encoding accessory and regulatory proteins (*ure*D, *ure*E, *ure*F, *ure*G and *ure*R). This plasmid was used as template to clone each of the structural genes *ure*A, *ure*B and *ure*C, which encode the subunits γ, β and α, respectively.

Primers used to amplify *P. mirabilis ure*A 5-CATATGGAATTAACACC AAGAGAA-3, 3-AGATCTCCTACACAATAGGTGAGTGAATTG-5, *P. mirab ilisure*B 5-CATATGTAATAACATGATCCCCGGTG-3, 3-AGATCTTTTTT CTCACT CTCCAATTTACCC-5 and *P. mirabilis ure*C 5-CATATGAA AACTATCTCACGTCA AGCTT-3, 3-AGATCTCGCTGGTTAAAATAAGAA ATA GCG-5 were designed based on *P. mirabilis* HI4320 genome (http://www.ncbi.nlm.nih.gov/genome/?term=proteus+mirabilis). Each insert was subcloned into the vector pGEM T-Easy (Promega, Madison, WI, USA) and transformed into *E. coli* XL10-Gold ultracompetent cells (Novagen, Madison, WI, USA) to amplify and maintain the plasmid. The Zyppy™ Plasmid Miniprep kit (Zymo Research Corp, Irvine, CA, USA) was used for plasmid purification which was then cleaved by restriction enzymes (Promega, Madison, WI, USA), both steps performed as indicated by the manufacturers. All inserts were cloned into a pET15-b in which a Streptag II sequence was inserted [21]. Finally, *P. mirabilis* pET15b::*ure*A plasmid was transformed into *E. coli* BL21 (DE3) pLysS (Novagen, Madison, WI, USA), whereas the plasmid pET15b::*ure*B and pET15b::*ure*C for expression of *P. mirabilis ure*B and *ure*C genes, respectively, was achieved using *E. coli* Arctic Express (DE3) (Novagen, Madison, WI, USA).

Alternatively, *ure*B gene was also cloned in plasmid pET23a, between *Nde*I and *Xho*I restriction enzymes (produced by GenScript, Piscataway, NJ, USA). The plasmid pET23a::*ure*B was transformed in *E. coli* (Lemo21) in order to obtain the expression of ureB subunit in the soluble fraction, as will be discussed in the manuscript.

2.2. Bacterial growth and induction conditions

2.2.1. Proteus mirabilis urease (PMU)

Escherichia coli HB101 cultures were performed in LB, 100 $\mu g.mL^{-1}$ ampicillin (Sigma-Aldrich, St. Louis, MO, USA) and 1 μM $NiCl_2$ under constant agitation (185 rpm) at 37 °C. The induction of urease expression was carried out by addition of 500 mM urea for 3 h, as soon as the culture reached OD_{600} of 0.7. Screening of recombinant colonies expressing ureolytic activity was performed by urea segregation agar methodology [23].

2.2.2. PMU structural subunits

All cell cultures were carried out using LB medium with 100 $\mu g.mL^{-1}$ of ampicillin (Sigma-Aldrich, St. Louis, MO, USA). For pET15b::*ure*A and pET23a::*ure*B plasmid, 36 $\mu g.mL^{-1}$ of chloramphenicol (Sigma-Aldrich, St. Louis, MO, USA) were added, while for pET15b::*ure*B and pET15b::*ure*C-expressing cultures, 20 $\mu g.mL^{-1}$ of gentamycin were added. Cultures were performed at 37 °C, under constant agitation (180 rpm). Protein expression was induced by addition of 0.5 mM IPTG when the cellular growth achieved an OD_{600} of 0.7. Cell cultures were kept overnight at 27 °C for *ure*A and 18 °C for *ure*B and *ure*C to allow protein synthesis.

2.3. Crude extract and purification of PMU

The recombinant holoprotein encoded by the plasmid carrying the whole urease operon was called PMU. The recombinant subunits were designated PmUreγ, PmUreβ and PmUreα, encoded by the plasmids carrying the *ure*A, *ure*B and *ure*C genes, respectively.

After bacterial growth, the culture was centrifuged at 5800 × *g* for 15 min at 4 °C. The pellet was ressuspended in PEB [20 mM sodium phosphate pH 7.5, 1 mM EDTA, 5 mM β-mercaptoethanol] and centrifuged. To remove excess of urea from the pellet, the process was repeated three more times. Cells were suspended in PEB buffer and disrupted using a Unique Ultrasonic Homogenizer (Hielscher Ultrasonics, Teltwon, Germany), 10 pulses of 50 s, in ice bath. After lysis, the material was centrifuged at 23,000 × *g* for 60 min at 4 °C and the supernatant was dialyzed exhaustively to remove the urea still present in the solution.

After dialysis, the crude extract was submitted to three sequential chromatographic steps. The extract was applied into a HiTrapQ™ column (GE Healthcare, Little Chalfont, UK), at 60 % of its protein binding capacity. The resin was equilibrated with PEB pH 7.5 and washed with the same buffer to remove unbound proteins. The fraction with ureolytic activity was eluted stepwise in PEB pH 7.5 containing 400 mM KCl. The urease-enriched fractions were pooled and dialyzed against PEB pH 7.5 and then loaded into a Q-Sepharose™ column (GE Healthcare, Little Chalfont, UK) mounted in an ÄKTA chromatography system (GE Healthcare, Little Chalfont, UK), equilibrated in the same buffer. Elution was performed with a linear gradient from 0 to 600 mM KCl in PEB 7.5. The active fractions were pooled, concentrated using an Amicon device with a cut-off of 30 kDa (Merck Millipore, Darmstadt, Germany) and then further purified by size exclusion chromatography (Superdex 200™ 26/60-pg), equilibrated in PEB buffer pH 7.0. Before each bioassay, the solution of PMU was sterilized by passing through 0.22 μm syringe filters.

2.4. Crude extract and purification of PMU subunits

After bacterial growth, the culture was centrifuged at 5800 × *g* for 10 min at 4 °C. The pellet was suspended in buffer containing 100 mM Tris–HCl pH 8.0, 150 mM NaCl and 1 mM EDTA. Cells were disrupted by sonication in ice bath, 15 cycles of 1 min at 20 kHz. Cellular debris were pelleted by centrifugation at 14,000 × *g* for 30 min. PmUreγ was found

in the culture supernatant whereas the other two proteins were expressed as inclusion bodies, using the plasmid pET 15b. To solubilize PmUreβ and PmUreα, cellular debris were washed three times with Tris–HCl, containing 3 % (v/v) Triton X-100, followed by three washes with Tris–HCl without Triton X-100. After washing and centrifugation, the pellets were suspended in 6 M urea, and kept under agitation, overnight at 4 °C. After solubilizing proteins, urea was removed by dialysis and any precipitated material still present was removed by centrifugation at 14,000 × *g* for 20 min. After the protein refolding procedure, crude extracts of PmUreβ and PmUreα were obtained. The crude extracts were then subjected to an affinity chromatography step using StrepTactin resin (GE Healthcare, Little Chalfont, UK) equilibrated in 100 mM Tris–HCl pH 8.0, 150 mM NaCl, 1 mM EDTA, and elution was carried out by addition of 2.5 mM D-desthiobiotin to the eluent. Before each bioassay, a gel filtration step in Superose 6 10/300 column (GE Healthcare, Little Chalfont, UK) was conducted to change the solvent to 50 mM Tris–HCl pH 7.5 buffer.

The PmUreβ cloned in pET23a and expressed in *E. coli* (Lemo21) the culture was centrifuged at 5800 × *g* for 10 min at 4 °C. The pellet was suspended in buffer containing 50 mM Tris–HCl pH 7.5, 500 mM NaCl and 20 mM imidazol. The cells were disrupted by sonication and cellular debris were pelleted by centrifugation at 14,000 × *g* for 30 min. PmUreβ was found in the culture supernatant. This subunit, containing a His tag in the C-terminal portion of the protein were then subjected to an affinity chromatography using Chelating Sepharose resin (GE Healthcare, Little Chalfont, UK) equilibrated in 50 mM Tris–HCl pH 7.5 buffer, 500 mM NaCl and 20 mM of imidazole. The column was washed with the same buffer containing 70 mM imidazole and then eluted with 500 mM of imidazole.

Before each bioassay, a dialysis was conducted to change the solvent to 10 mM Tris–HCl pH 7.5 buffer and 1 mM DTT. Solutions of PMU subunits were sterilized by passing through 0.22 μm syringe filters.

2.5. Protein determination

The protein contents were determined by absorbance at 280 nm or by the Bradford method [24] using bovine serum albumin as standard.

2.6. SDS-PAGE

SDS-PAGE was performed according to [25]. The material was diluted in sample buffer, heated to 95 °C for 5 min and applied in 12 or 15 % polyacrylamide gels. Native-PAGE was performed in 7.5 % polyacrylamide gels, without SDS and reducing agents, and without boiling the samples. The gels were stained with colloidal Coomassie Brilliant Blue or silver nitrate.

2.7. Urease assay and zymography

Urease activity was determined in 96 well plates (Thermo Scientific, Waltham, MA, USA) in 100 μL final reaction volume of 20 mM sodium phosphate pH 7.5, 150 mM NaCl containing 100 mM urea and the tested sample. The enzymatic reaction proceeded for 30 min at 37 °C and the color reaction was developed using the phenol-nitroprussiate method [26]. Zymography in native-PAGE gels was carried out by the nitroprusside-thiol reaction according to [27].

2.8. Platelet aggregation

Peripheral human blood of healthy volunteers was collected in presence of 0.313 % (w/v) sodium citrate. The blood samples were centrifuged at 400 × *g* for 10 min at 25 °C to obtain a platelet-rich plasma (PRP). All procedures regarding blood collection and handling were conducted in strict accordance with Brazilian legislation (Law no. 6.638/1979) and approved by the institutional Ethics Committees (UFRGS 721.217; PUCRS 14/00414).

2.8.1. Platelet aggregation assay by microscopy

PMU subunits were incubated with a platelet rich plasma (PRP) for 1 h at room temperature on a rocking platform. After centrifugation, the pelleted cells were fixed with 4 % v/v formaldehyde, and the aggregates were counted in a Neubauer chamber using an optic microscope (Carl Zeiss Microscopy, Thornwood, NY, USA). An aggregate was defined as a cluster of five or more platelets grouped together. The methodology was based and adapted from [28].

2.9. Yeast proliferation assay

2.9.1. PMU and subunits

Candida albicans and C. parapsilosis (kindly provided by Dr. Valdirene Gomes, Universidade Estadual do Norte Fluminense, Campos dos Goytacazes, RJ, Brazil) were grown for 48 h on Sabouraud agar (1 % peptone, 2 % glucose and 1.7 % agar-agar) at 28 °C. After growth, the cells were harvested, transferred to sterile saline (0.9 % NaCl), counted and 10^4 cells were placed on 96 wells plates (Thermo Scientific, Waltham, MA, USA), containing Sabouraud broth. After addition of tested proteins in concentration of 33 and 65 $\mu g.mL^{-1}$ for PMU (molar concentrations of 120 and 140 nM respectively) and 22 and 65 $\mu g.mL^{-1}$ for subunits (molar concentrations: PmUreγ, 2 and 6 μM; PmUreβ, 1.8, 2.25, 4.5, 5 and 9 μM); PmUreα: 0.33 and 1 μM, respectively), the yeasts were incubated 24 h at 28 °C. To assess cell viability, colony forming units (CFU) were determined after further incubation at 28 °C for 24 h in Sabouraud agar plates by the drop plate method [9].

2.10. Optical microscopy

Candida albicans were grown for 24 h on Sabouraud agar (1 % peptone, 2 % glucose and 1.7 % agar-agar) at 28 °C. After growth, the cells were resuspended in Sabouraud broth (1 % peptone, 2 % glucose), counted and 10^4 cells were placed on 96 wells flat bottomed plates (Thermo Scientific, Waltham, MA, USA), and grown during 24 h at 28 °C. Then the cells were incubated with 9 μM of PmUreβ and/or buffer (10 mM Tris–HCl pH 7.5 buffer and 1 mM DTT) during 3 h at 28 °C. To evaluate yeast morphology and aggregation, 20 μL of each sample were dropped on a Neubauer chamber, and examined under an optic microscope (Carl Zeiss Microscopy, Thornwood, NY, USA). A yeast aggregate was defined as a cluster of five or more *C. albicans* grouped together.

2.11. Scanning electron microscope (SEM)

After the incubation period, the culture medium was centrifuged, washed with buffer, then the cells were fixed with glutaraldehyde (2.0 %) over seven days, after that the samples were washed for 30 min to remove the glutaraldehyde, followed by drying at room temperature. Controls consisted of yeast samples only, with no additions. Specimens were dehydrated in baths with increasing concentrations of acetone (50 %, 70 %, 90 % and 100 %) for 10 min each. Specimens were dried, metallized and stored in desiccator for subsequent observation by MEV (Zeiss Evo MA10 - German) [29].

2.12. Bioassays with insects

Fifth-instar nymphs of the kissing bug *R. prolixus* (a Chagas' disease vector) were kindly provided by Dr. Denise Feder (Universidade Federal Fluminense, Niteroi, RJ, Brazil). The insects were kept on a light:dark cycle of 12 h/12 h, temperature of 27 ± 1 °C and 60 % relative humidity. The cotton stainer bug *D. peruvianus* were from a colony established in our laboratory, maintained at 23 °C and 75 % of relative humidity, with light-dark cycle of 16 h:8 h, and fed *ad libitum* on cotton seeds. *N. cinerea* cockroaches were from our own breeding colony, kept at 22–25 °C, with a light:dark cycle of 12 h/12 h, food (Birbo Premium Meat & Vegetables) and water *ad libidum*.

2.12.1. Interaction of PMU with R. prolixus' central nervous system (CNS)

PMU (63 nM) or bovine serum albumin (BSA, 63 nM) were incubated with Texas Red (0.5 mg/mL) during 1 h, at 4 °C, with continuous stirring [31]. The samples were then exhaustively dialyzed against 20 mM NaPB, pH 7.0 to remove any excess of free dye. Fifth-instar nymphs were anesthetized by cooling at −20 °C for 5 min, immobilized ventral side down and their body cavities were opened. The CNS, composed by brain and ganglia, was dissected. Incubation of the CNS was carried out with 63 nM solutions of Texas Red-labeled PMU or Texas Red-labeled BSA for 1 h at room temperature, followed by three washes with buffer (30 min each) at room temperature. The CNS were then placed in coverslips and visualized under an inverted microscope Eclipse TE2000-S (Nikon, Tokyo, Japan), equipped with an ORCA-ER-1394 Camera (Hamamatsu Photonics KK, Hamamatsu, Japan), and with Phylum 4.2.0 (Improvision, Lexington, MA, USA) as image acquisition software. The methodology was adapted from [31].

2.12.2. Nitric Oxide Synthase (NOS) assay in N. cinerea's CNS homogenates

For these experiments, the CNS of adult cockroaches was dissected as described above and homogenized in 20 mM Tris–HCl (pH 7.4), 0.32 M sucrose, 2 mM Na_2EDTA, 2 mM DTT and 10 % protease inhibitors (Sigma Chem. Co.). The homogenates were centrifuged (10,000 × *g*, 10 min, 4 °C) and the protein concentration was determined by the Bradford dye method. The homogenates were incubated at 4 °C for 1 h with 63 nM PMU or buffered saline (137 mM NaCl, 2.7 mM KCl, 10 mM Na_2HPO_4, 2 mM KH_2PO_4, pH 7.5) as control. NOS activity was measured by incubating the samples at 37 °C in a reaction mixture containing 50 mM NaPB (pH 7.0), 1 mM $CaCl_2$, 1 mM L-arginine, 100 μM NADPH, 10 μM DTT, 0.1 μM catalase, 4 μM superoxide dismutase (SOD) and 5 μM oxyhemoglobin, as described in Galvani et al. 2015 [32]. Formation of methemoglobin was monitored at 401 nm. Negative controls were done carrying out the reaction in the presence of the NOS inhibitor, NG-methyl-L-arginine (L-NMMA, 1 mM).

2.12.3. In vitro hemocyte aggregation assay

Fifth-instar nymphs of *R. prolixus* were sterilized by immersion in ethanol 70 %, and their hemolymph was then collected from a cut in one leg with a micropipette. A hemolymph pool (7 insects) was mixed in a proportion of 1:1 (v/v) with *Rhodnius* saline as reported by [33]. The diluted hemolymph was incubated with PMU subunits (final concentrations of 2.2 μg mL^{-1}) and incubated at room temperature for 1 h on a rocking platform. The aggregates were counted in a Neubauer chamber using an optic microscope (Carl Zeiss Microscopy, Thornwood, NY, USA). A hemocyte aggregate was defined as five or more cells clamped together. In order to assess the relevance of divalent cations in the process of hemocyte aggregation, experiments were performed in presence of 100 μM EDTA, following the same protocol. The experiments were performed in quadruplicates.

2.12.4. Lethality assay by injection into D. peruvianus

D. peruvianus fifth-instar nymphs (~30 mg body weight each) were anesthetized by cooling at 4 °C for 5 min, immobilized onto a plate and injected into the hemocoel with 5 μL of solutions (163 μg.mL^{-1}) of PmUreγ, PmUreβ or PmUreα in 50 mM Tris pH 7.5 (~27 ng of protein. mg^{-1} insect body weight), with a Microliter 900 series syringe (Hamilton, Reno, NV, USA). Controls received injections of buffer alone [30]. The experiments were performed in triplicates of groups of 5 insects. Mortality rates were recorded every 24 h for 3 days.

2.12.5. Lethality assay by oral administration to D. peruvianus

Fifth-instar nymphs of *D. peruvianus* were immobilized on a flat surface and their mouth apparatus were introduced into a glass capillary containing 5 μL of test solution, as described in [30]. The experimental groups were fed with the solutions (163 μg mL^{-1}) of PmUreγ, PmUreβ or PmUreα dissolved in 50 mM Tris–HCl pH 7.5, to give final doses of ~27 ng of protein per mg of insect body weight. The controls fed with Tris–HCl buffer alone. The experiments were performed in triplicates using groups of 5 insects. Mortality rates were recorded every 24 h for 3 days.

2.13. Protein sequence analyzes

Protein sequences (for bacterial urease subunits, plant urease, and Jaburetox) were collected from NCBI - Protein database [34] and aligned using the Clustal Omega algoritm [35]. Internal amino acid sequence repeats related to genetic duplication were inspected with Swelfe [36]. Ancestral state reconstruction was carried out with MEGA7 [37], (http://www.megasoftware.net/) using the previously published urease phylogeny data as reference [38].

2.14. Molecular modeling and dynamics

The molecular model for the PmUreβ subunits was built with Modeller 9 [39] (https://salilab.org/modeller/) using the *Sporosarcina pasteurii* urease structure (PDB ID 4AC7 [40] as template. Molecular dynamics simulations were carried out with the Gromacs 4 suite [41], (http://www.gromacs.org/) following protocols for native, physiological conditions [38], and for structural stability assessment [42].

3. Results

3.1. Recombinant PMU and its recombinant isolated subunits

A plasmid carrying the whole operon of PMU, consisting of *ureR*, *ureD*, *ureA*, *ureB*, *ureC*, *ureE*, *ureF* and *ureG* genes [43], was employed to produce the protein in *Escherichia coli*. In the absence of a tag to aid purification, conventional chromatographic steps were performed to obtain the enzymatically active recombinant PMU. The homogeneity of purified PMU was assessed by native-PAGE and zymograms confirming its ureolytic activity (Suppl. Fig. 1).

To obtain PMU's isolated subunits, pET15b plasmids encoding each protein were constructed. Recombinant PmUreγ was found in the *E. coli* soluble fraction, while PmUreβ and PmUreα were produced as inclusion bodies. Alternatively, the PmUreβ subunit was cloned in *E. coli* strain Lemo21 (DE3) using pET23a vector, due the low solubility, then the PmUreβ subunit was found in the soluble fraction after cells lysis. No differences in the biological effects were observed between the two versions of PmUreβ. (Suppl. Fig. 2).

3.2. Moonlighting properties of PMU and of its isolated subunits

3.2.1. Toxicity of PMU and isolated subunits against yeasts

The antifungal activity of PMU was tested on two *Candida* species. Incubation for 24 h with PMU at 33 and 65 μg.mL^{-1} (120 and 240 nM, respectively), led to a dose-dependent decrease of the proliferation rates of *C. parapsilosis* (Fig. 1B), but this inhibition was not observed to *C. albicans* (Fig. 1A). PMU's isolated subunits were tested on *C. albicans* and *C. parapsilosis* (Fig. 1C and D). Proliferation rates of *C. albicans* and *C. parapsilosis* decreased in the presence of 65 μg.mL^{-1} PmUreβ (corresponding to 5.3 μM), but not with the other subunits in the tested concentrations.

Among the subunits, PmUreβ proved to be more promising regarding antifungal activity. With this evidence, we decided to evaluate other concentrations (2.25 μM, 4.5 μM and 9 μM) of PmUreβ on *C. albicans* (Fig. 2). We decided to use *C. albicans* in this study because it is an attractive yeast model used frequently in antifungal studies [44].We observed higher susceptibility of *C. albicans*, highlighting the concentrations of 4.5 μM and 9 μM of PmUreβ. The 2.25 μM concentration is less active, but still decreased the viability of *C. albicans*.

In order to understand how PmUreβ acts against *C. albicans*, we performed optical microscopy (magnification 200 X) after 3 h of treatment with the highest dose (9 μM) and observed the formation of yeast

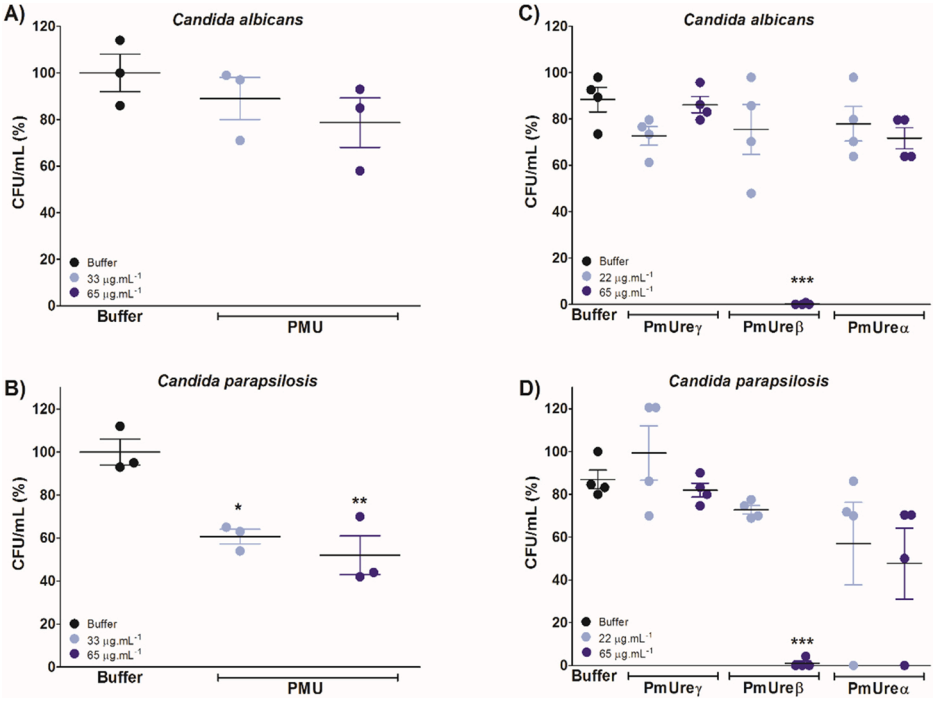

Fig. 1. Antifungal effect of *Proteus mirabilis* urease (PMU) and of its subunits on yeasts. Panels A-B. Recombinant PMU (33 and 65 µg.mL^{-1}, 120 and 240 nM respectively) was incubated for 24 h at 28 °C with the yeasts and then colony-forming units (CFU) were determined by the drop plate method. Panels C-D. Yeasts were incubated with PMU's subunits (22 and 65 µg.mL^{-1}) for 24 h at 28 °C and then CFU were determined by the drop plate method. Molar concentrations: PmUreγ, 2 and 6 µM; PmUreβ, 1.8 and 5 µM; PmUreα: 0.33 and 1 µM, respectively. Buffer, 50 mM Tris–HCl, pH 7.5. Results are represented as percentage of the number of CFU.mL^{-1} observed for the negative control (no treatment). Results are means ± S.E.M, N = 3, * $p \leq 0.05$; ** $p \leq 0.02$; *** $p \leq 0.01$.

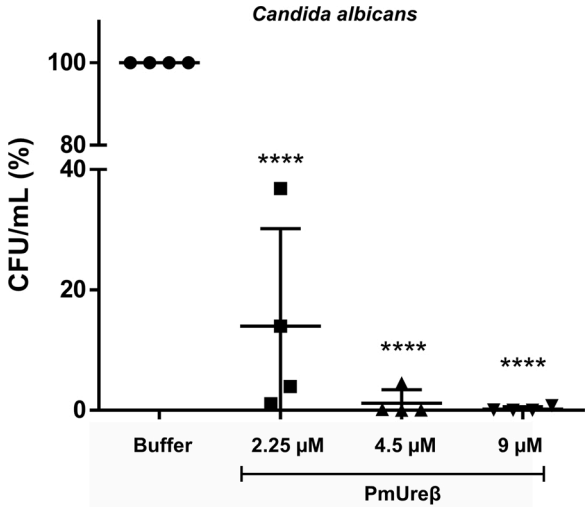

Fig. 2. Dose-effect curve of antifungal effect of PmUreβ on *C. albicans*. Yeasts were incubated with PmUreβ (2.25, 4.5 and 9 µM) for 24 h at 28 °C, then colony-forming units (CFU) were determined by the drop plate method. Buffer (10 mM Tris–HCl pH 7.5 buffer and 1 mM DTT). Results are represented as the number of CFU.mL^{-1} observed for the negative control (no treatment). Results are means ± S.E.M, N = 4, * $p \leq 0.05$; ** $p \leq 0.02$; *** $p \leq 0.01$.

aggregates in the samples treated with PmUreβ in comparison with the control (Fig. 3).

The formation of aggregates was confirmed by scanning electron microscopy (SEM) (Magnification 3000 X) (Fig. 4). When we prepared the samples to SEM; however, it was not possible to observe enough cells upon treatment with either 9 µM and 4.5 µM PmUreβ, only isolate and highly damaged cells. Then, we perfomed the treatment with 2.25 µM and an altered phenotype of the treated yeasts, a flocculent extracellular material was observed by the electron microscopy, connecting cells. (Fig.4C). It is important to highlight that the reducing agent (DTT), fundamental to protein stabilization, alone was not toxic to the cells (Fig.4B), since the effect was compared against yeast grown in saline (Fig.4A) and no changes in yeast morphology were observed.

3.2.2. *Neurotoxicity of PMU in insects*

Here we show that PMU bound to *R. prolixus* nervous ganglia (Fig. 5C) and, at a concentration of 63 nM, it inhibited ~40 % the nitric oxide synthase activity of *N. cinerea*'s central nervous system (CNS) homogenates (Fig. 5D).

3.2.3. *Insecticidal activity of PMU's subunits*

The cotton stainer bug *Dysdercus peruvianus* was employed to investigate the insecticidal effect of PMU's subunits (Fig. 6A-B). PMU's subunits were insecticidal upon injection (*ca.* 27 ng protein.mg^{-1} body weight), and lethality was seen for PmUreα and PmUreγ, with the latter promoting the highest mortality (Fig. 6A). The same dose of the subunits tested orally in *D. peruvianus* induced a dose- and time-dependent lethal effect. PmUreβ produced the highest lethality (90 %) whereas PmUreα (which contains the enzyme's active site) given orally to *D. peruvianus* did not induce significant mortality after the observed period (Fig. 6B).

JBU and Jaburetox were shown to modulate *R. prolixus* immunity by inducing hemocyte aggregation *in vitro*, through a cation-dependent mechanism [28,45]. In this work, we conducted a similar *in vitro* assay incubating hemocytes of the kissing bug *R. prolixus* with PMU's subunits and analyzing its capacity to induce aggregation, thus indicating the activation of a cell immune response. Fig. 6C shows that, when PMU's subunits were tested at 2.2 µg.mL^{-1} concentrations, PmUreβ (180 nM) and PmUreγ (200 nM) induced a significant increment in the number of hemocyte aggregates when compared with the control incubated with vehicle. PmUreα (33 nM) had no effect on the aggregation response of *R. prolixus* hemocytes *in vitro*. In all tested cases, the incubation with the chelating agent EDTA reverted the aggregation process, evidencing that divalent cations are needed for this immune response (Fig. 6C).

3.2.4. *Aggregation of human platelets by PMU and its subunits*

One of the effects that convey pro-inflammatory properties to ureases is their ability to activate blood platelets, coupled to exocytosis of their dense granules [46–48], and conversion of these cells into a pro-inflammatory phenotype [15]. PMU (17 µg.mL^{1}, 63 nM) was found

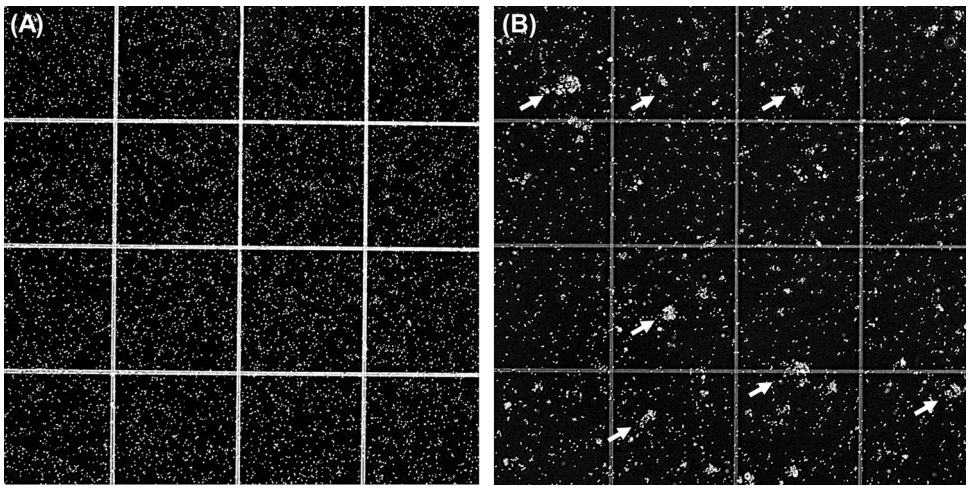

Fig. 3. Optical microscopy of *C. albicans* after 3 h treatment with PmUreβ. A) saline; B) 9 μM PmUreβ. Each sample were dropped on a Neubauer chamber, and examined under an optic microscope (Carl Zeiss Microscopy, Thornwood, NY, USA). A yeast aggregate was defined as a cluster of five or more *C. albicans* grouped together. In B the *C. albicans* cell aggregation could be observed (arrows). Magnification 400 X.

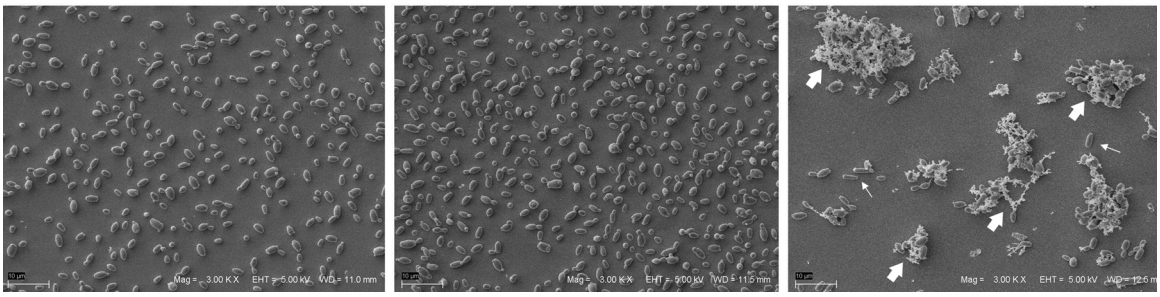

Fig. 4. Scanning Electron Microscopy of *C. albicans* after 24 h assay in A) saline solution (NaCl 0.9 %); B) buffer 10 mM Tris–HCl pH 7.5 buffer and 1 mM DTT; C) 2.25 μM of PmUre*β* in the same buffer as in panel B. In A and B the *C. albicans* cells display a typical oval shape. In panel C the cells are more elongated (thin arrow) and are involved by a flocculent extracellular material disposed as a network (large arrow). Magnification 3000 × .

also able to induce aggregation of human platelets [22]. PMU-induced aggregation had a slower rate compared to the platelets' response to the physiological agonist ADP (20 μM), and a similar extent of aggregation was eventually reached [22].

Microscopic observation allowed visualization of the small platelet aggregates formed in the presence of PMU's subunits (Fig. 7). PmUreβ produced significantly more and bigger platelet aggregates than did PmUreγ or PmUreα (Fig. 7A and B). In contrast, our previous studies with isolated subunits of *H. pylori*'s urease indicated that only its B subunit, which is equivalent to PmUreα, is able to induce aggregation of platelets [15].

3.3. Topology of PmUre*β* in PMU and molecular dynamics

Fig. 8 shows the molecular model constructed for PMU. As depicted for Jaburetox in JBU [49], PmUreβ is also well exposed at the protein's surface. Molecular dynamics simulations (Fig. 8C to E) were performed to inspect PmUreβ for possible disordered behavior, as seen for Jaburetox [50] and Soyuretox [10]. Loss of secondary structure was observed after 100 ns under physiological conditions, with ~36 % of secondary structure elements remaining after the simulation (Fig. 8D). At a higher temperature (to evaluate structural stability), a complete loss of secondary structure elements was observed (Fig. 8E), supporting a tendency of structural disorder for PmUreβ.

3.4. Gene or segment duplication in ureases

The fact that PmUreβ displayed all the activities tested here, paralleling the biological properties of Jaburetox, besides also exhibiting a platelet-aggregating effect, was quite unexpected. Jaburetox corresponds to positions 230–321 in the sequence of JBURE-II, the isoform of JBU that served as template to clone the peptide [8]. In an attempt to understand these results, PMU was inspected for internal sequence repeats, to detect possible duplications of functionally relevant regions. The amino acid sequence of PmUreγ, PmUreβ and PmUreα are collinear to segments 1–100, 131–238, and 271–840 of the JBU molecule, respectively (Fig. 9). Two similar segments were identified in the region between PmUreβ and PmUreα, when comparing PMU and the prototypical JBU as reference (Fig. 9). One similarity pair encompasses a "jaburetox-like" segment in PmUreα (aligning to amino acid positions 268–316 in JBU) and its homologous in PmUreβ (177–229 in JBU), as shown in Fig. 9A. The second pair encompasses (Fig. 9A) a segment in PmUreα corresponding to 307–331 in JBU and its homologous in PmUreβ (186–210 in JBU). Alignment of these regions to their putative ancestor sequences revealed their evolutionary conservation (Fig. 9B).

4. Discussion

The well recognized role of PMU as a virulence factor of *P. mirabilis* has been so far exclusively attributed to its enzyme activity. Here our

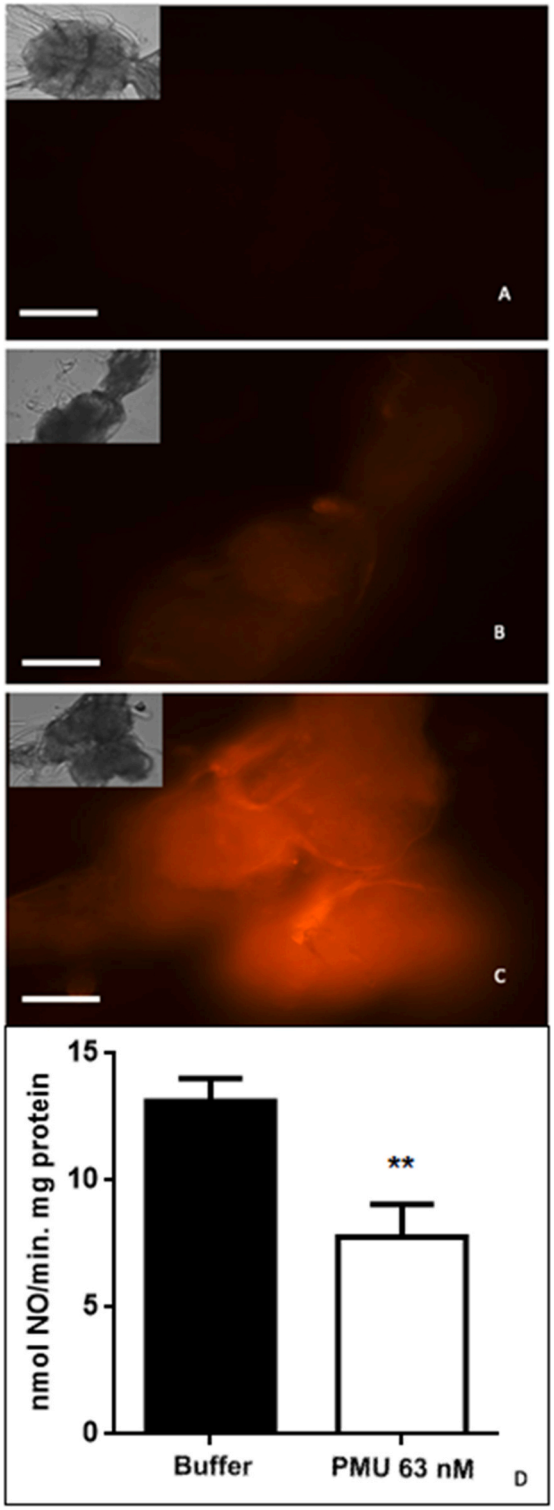

Fig. 5. Neurotoxicity of *Proteus mirabilis* urease (PMU) to insects. Panels A, B and C. Binding of PMU to central nervous system (CNS) of *R. prolixus*. Dissected CNS were incubated for 1 h with phosphate buffer saline (PBS) (A), Texas Red-labeled bovine serum albumin (BSA), 63 nM (B) or Texas Red-labeled PMU, 63 nM (C) and analyzed by fluorescence microscopy. Scale-bars: 200 μm. Insets show the same fields under bright field microscopy. The pictures show representative experiments of at least three independent assays. Panel D. Inhibition by PMU of nitric oxide synthase activity of *N. cinerea*'s CNS. Homogenates were incubated with 63 nM PMU or buffer (control) for 1 h, on ice, and then nitric oxide synthase (NOS) activity was determined using L-arginine as substrate. The results are expressed as means ± S.E.M, N = 10, ** $p < 0.0032$.

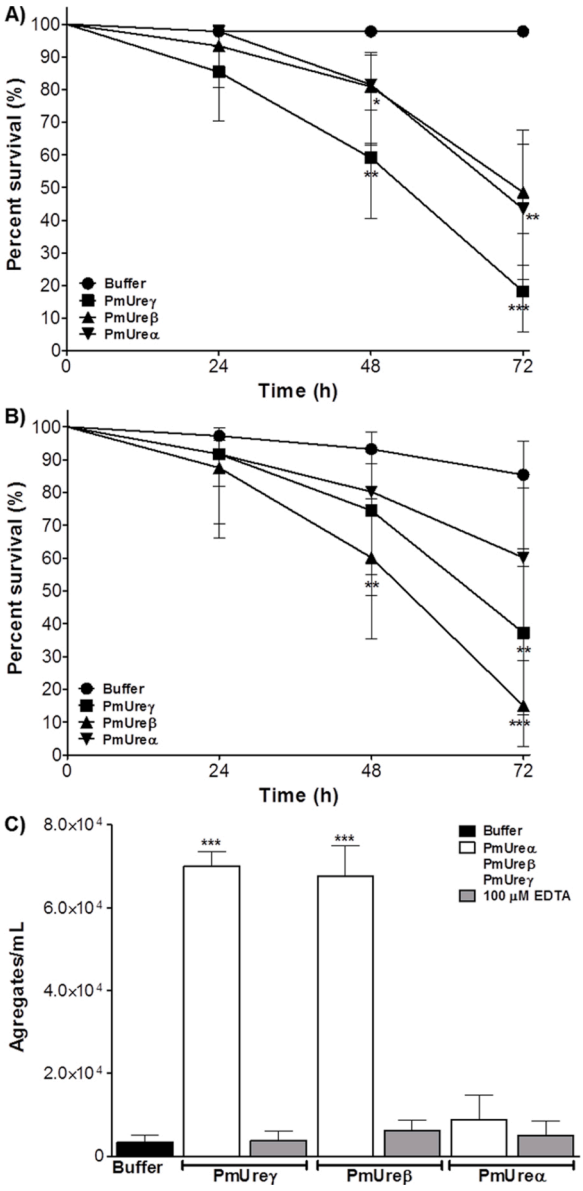

Fig. 6. Entomotoxicity of the isolated subunits of *P. mirabilis* urease (PMU). Panel A. Survival rates of *D. peruvianus* after hemocoel injection of 5 μL buffer (50 mM Tris–HCl pH 7.5; negative control) or 5 μL solutions of PMU's subunits, to give doses of 0.27 ng of per mg of insect body weight. Results are means ± S.E.M, N = 3. ** $p \leq 0.02$; *** $p \leq 0.01$. Panel B. Survival rates of *D. peruvianus* fed on 5 μL buffer or 5 μL solutions of PMU's subunits, to give doses of 0.27 ng of per mg of insect body weight. Results are means ± S.E.M, N = 3. ** $p \leq 0.02$; *** $p \leq 0.01$. Panel C. *R. prolixus* hemocyte aggregation induced by PMU's subunits. Open bars indicate the number of hemocytes aggregates formed *in vitro* after 1 h incubation of insect hemolymph with PMU's subunits at 2.2 μg. mL^{-1} (PmUreγ: 200 nM, PmUreβ: 180 nM, PmUreα: 33 nM) in 50 mM Tris–HCl, pH 7.5. Hatched bars show the number of aggregates formed when 100 μM EDTA was added to the solutions of PMU's subunits. Control (black bar) hemocyte aggregation was carried out in buffer alone.

data revealed that PMU is a true moonlighting protein that carries several other biological properties unrelated to ammonia production. Particularly, the exocytosis-inducing effect that underlies the aggregation response of platelets to ureases [4], observed here with nanomolar doses of PMU, and which correlates to the pro-inflammatory activity of these proteins [15,51,52], could be relevant in the context of the diseases caused by *P. mirabilis*.

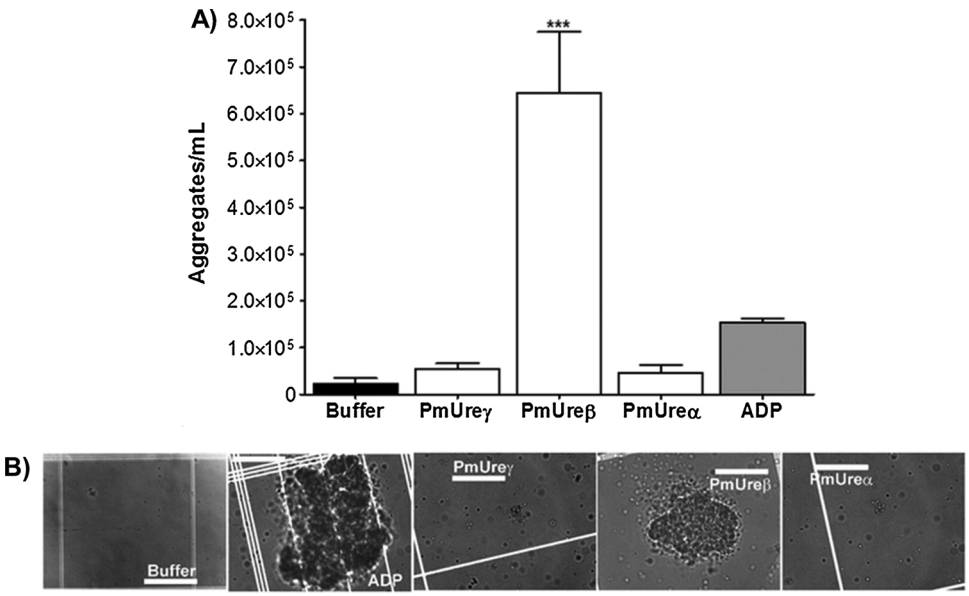

Fig. 7. Aggregation of human platelets induced by *P. mirabilis* urease (PMU) and its isolated subunits. The reaction started by addition of PMU's subunits or ADP to a platelet-rich plasma suspension (PRP) and the aggregation response was monitored. Panel A. PRP aliquots were incubated with PMU's subunits, buffer or ADP for 1 h on a rocking platform, then the samples were centrifuged, the pellets were fixed with formaldehyde and the number of aggregates was counted in a Neubauer chamber. PmUreγ (9.8 μM), PmUreβ (8.8 μM) and PmUreα (1.6 μM). Buffer: 50 mM Tris–HCl, pH 7.5. Panel B. Microscopic view of aggregates (defined as a cluster of 5 or more cells) as formed in the conditions described in panel B. Bar: 400 μm. Results are mean ± S.E.M, N=3, *** $p \leq 0.01$.

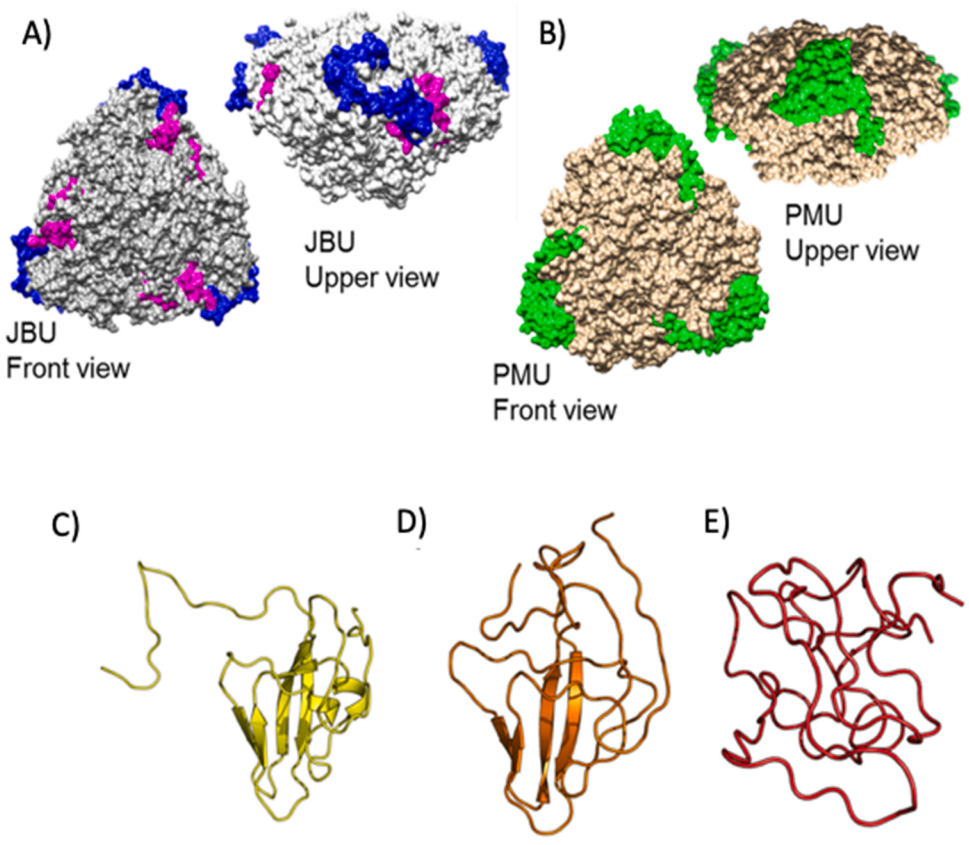

Fig. 8. Topology of PmUreb in *Proteus mirabilis* urease (PMU) and dynamics. Panels A and B. Trimeric forms of *Canavalia ensiformis* urease (JBU) (PDB 3LA4) and PMU (modeled), in front (left) and side (right) views. In panel A, jaburetox's N-terminal half is colored in blue and its C-terminal half in pink. In panel B, PmUreβ is depicted in green. Panels C, D and E. Conformations of PmUreβ and molecular dynamics simulations. In panel C, native PmUreβ (modeled); panel D, PmUreβ after 100 ns under normal conditions (310 K); panel E, PmUreβ after 100 ns under protein-disturbing conditions (498 K).

We first reported the non-enzymatic antifungal activity of ureases studying the effects of Canatoxin on filamentous phytopathogenic fungi [53], later followed by observation of fungitoxic effects of ureases from soybean and cotton seeds, and of *H. pylori*'s urease [54]. Postal and co-authors in 2012 described the fungitoxic effect of JBU and Jaburetox on yeasts [9]. As observed here for PMU, the protein inhibited *C. parapsilosis* proliferation in a similar concentration range as reported for plant ureases [4]. Interestingly, reports have shown that, when in the presence of *P. mirabilis*, there is a marked inhibition of biofilm formation by *C. albicans* [55] that could be due to PMU production. In our study we did not observe the inhibition of *C. albicans* growth by the holoprotein, in these tested concentrations. Biofilm studies will be conducted by our group with biofilm-producing *C. albicans* in order to confirm this hypothesis.

Concerning the subunits, PmUreβ inhibited proliferation of the yeasts, thus proving that PMU's fungitoxic effect does not require ureolysis. Since a region equivalent to Jaburetox is absent in bacterial ureases, our data confirmed the existence of more than one fungitoxic domain in

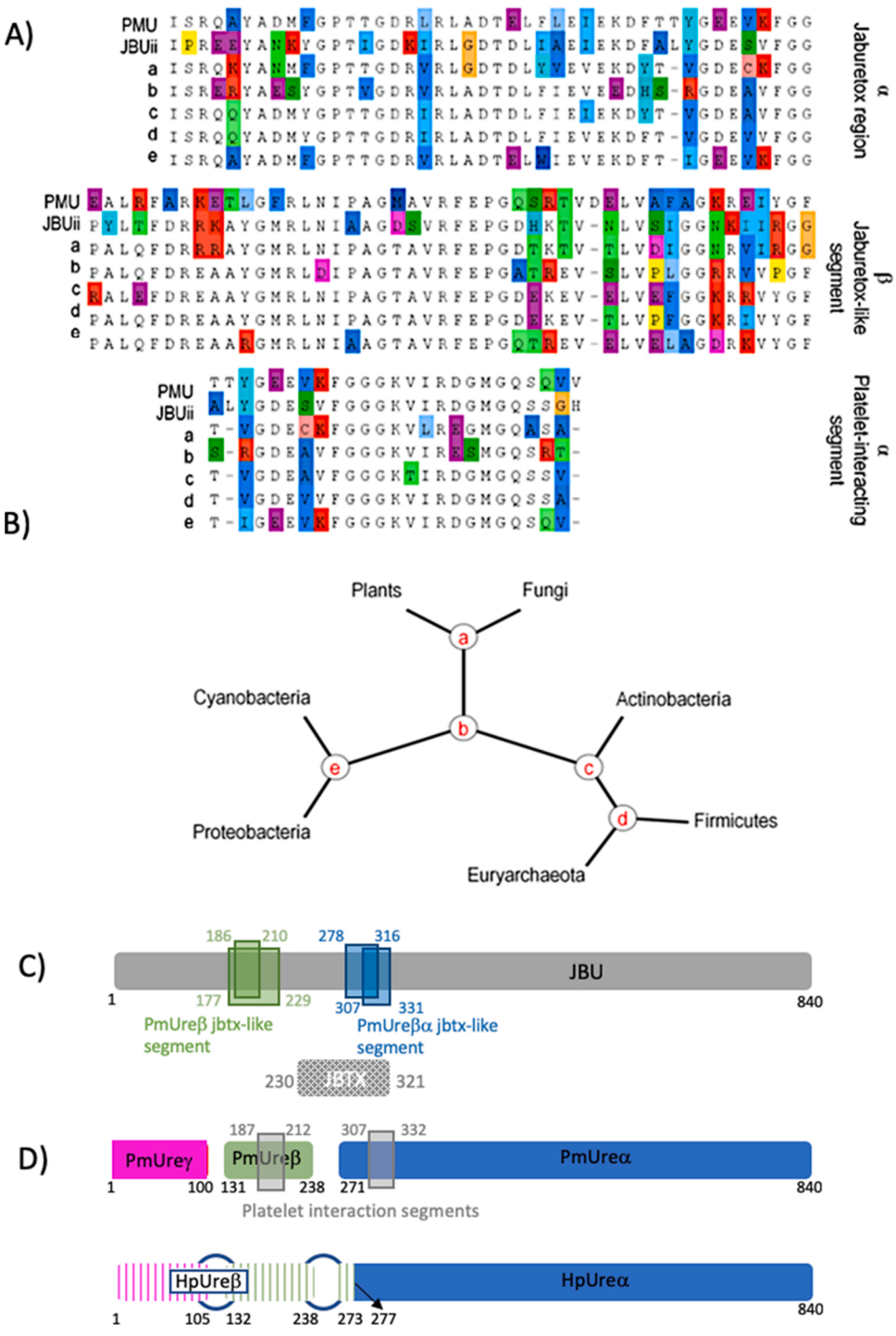

Fig. 9. Comparison of duplicated segments among ureases and their putative ancestors. Panel A. Alignments of "jaburetox-like" sequences in *C. ensiformis* JBURE-II urease (JBUii), PMU (*Proteus mirabilis* urease), and the most likely ancestor sequences, indicated as "a" to "e", for the nodes in the simplified phylogenetic tree shown in panel B (JBUii: ACL14297.1; PMU: WP_124740772.1, WP_109880188.1, WP_020945159.1; a-e: inferred in this study). Colors highlight differences from major consensus rule. Panels C and D. Schematic representation of *C. ensiformis* major urease (JBU), *P. mirabilis* (PMU) and *Helicobacter pylori* (HPU) ureases. In C) JBU single subunit (840 amino acids) is represented as a gray bar and jaburetox appears below in hatched gray. Duplications of jaburetox-like sequence in JBU and PMU (alignments shown in A) are represented as green and blue boxes, with numbers indicating amino acids positions. In D) PMU and its three subunits: PmUreγ (red), PmUreβ (green) and PmUreα (blue). Gray boxes in PMU identify its putative platelet-interacting segments (alignments shown in A). The numbers refer to the amino acid positions in JBU sequence. Below, HPU is shown with its UreA chain (HpUreβ) (striped red or green bars) and its UreB chain (HpUreα) (blue). Alignments of all sequences are presented in Suppl. Fig. 3.

ureases, as previously suggested by our group [4,9]. Unlike the effects observed to Jaburetox and Soyuretox, which induce the pseudohyphae growth [4,10], PmUreβ induced aggregation in *C. albicans* (Fig. 3B). In addition, the flocculent extracellular materials that were observed in the SEM (Fig. 4C), was already demonstrated in *C. parapsilosis* treated with baicalein in combination with fluconazole [56]. Regarding inhibitory concentration on *C. albicans*, PmUreβ proved to be effective at 2.25 μM (Fig. 2), comparable to the doses of Jaburetox and Soyuretox, 9 μM and 5 μM, respectively, needed to inhibit the growth of *C. albicans* [11]. Aggregation in *C. albicans* is an indicative of cell membrane or cell wall damage [57] providing an explanation of PmUreβ antifungal effect. The ability of Jaburetox to interact with fungal external cell membrane and/or cell wall was previously demonstrated [31]. Besides this, an initial study showed that Soyuretox was able to induce reactive oxygen species in *C. albicans* [10] although more studies are necessary to confirm it. Additional studies are under way aiming to understand the PmUreβ's mode of action against yeasts.

Our previous work on the entomotoxic properties of ureases focused mostly the single-chained plant proteins and the insecticidal effect was ascribed mainly to their "Jaburetox" moiety. However, tri-chained bacterial ureases, which lack a "jaburetox-like" sequence, can also be insecticidal, as reported for entomopathogenic *Photorhabdus* spp. [58] and *Yersinia pseudotuberculosis* [59] enzymes, implying that ureases contain more than one insecticidal domain.

Here, the neurotoxic effect of PMU in insects was established by its binding to *R. prolixus*' CNS tissues and by the pronounced inhibition of nitric oxide synthase activity of *N. cinerea*'s brain homogenates (Fig. 5). Similar bioassays have previously demonstrated the neurotoxic effects of Jaburetox in triatomine insects [32,60], and in *N. cinerea* cockroaches [31]. Furthermore, it has been shown that JBU affects insect behavior, heart frequency and muscle contraction [61], and interferes on the release of neurotransmitters by modulating insect calcium channels [62]. The evolutionary conservation of the nervous systems of invertebrates and vertebrates is reflected in the fact that many neurotoxins, ureases included, are active on both animal groups [63,64]. Mechanisms similar to those triggered by ureases in the nervous system of insects probably underlie the neurotoxicity and convulsant effect of Canatoxin [47,65] or that of *H. pylori* urease in rodents [66]. Thus, a potential contribution of PMU to neurological conditions such as neonatal meningitis [67] or adult meningitis following neurosurgery [68,69] deserves investigation. We have shown that ureases are neurotoxic to insects and impair their immune system, and similar effects were also observed for the urease-derived peptides Jaburetox and Soyuretox [1,4]. JBU and Jaburetox were found to bind to nervous tissues of the kissing bugs *Triatoma infestans* and *Rhodnius prolixus* [32] and of the cockroach *Nauphoeta cinerea* [31], accompanied by a pronounced inhibition of nitric oxide synthase activity in brain homogenates of these insects [32,60].

Studies on the structure *versus* entomotoxic activity were performed by testing PMU's subunits on *D. peruvianus,* a hemipteran susceptible to both, JBU and Jaburetox. All subunits were lethal to the insects, either injected or given orally, confirming the ureolysis-independent entomotoxicity of PMU (Fig. 5). PmUreγ was more toxic when injected, whereas PmUreβ administered orally promoted the highest toxicity. Besides neurotoxicity, JBU and Jaburetox also interfere on the immune response of *R. prolixus* and induce aggregation of the insect's hemocytes [1,4]. Hemocytes are granulocytes that combine biological properties of several types of mammalian leukocytes as well as of platelets [70]. Here, PmUreγ and PmUreβ, but not PmUreα, induced a cation-dependent aggregation of *R. prolixus* hemocytes thus ascribing an immunomodulatory component to PMU's entomotoxicity.

Plant and bacterial ureases, regardless of their enzymatic activity, promote platelet activation in the nanomolar range, by triggering an eicosanoid signaling cascade [4]. A platelet-activating effect was reported for liposaccharides extracted from *P. mirabilis* [71]. As the purity of the liposaccharide preparations was not described, it is not possible to exclude the presence of low amounts of PMU in that samples. Our group demonstrated that the recombinant PMU induced aggregation of human platelets in nanomolar concentrations, following a slower rate when compared to that prompted by the platelet agonist ADP (at a 317-fold greater dose) [22]. We described earlier that aggregation induced by HPU in rabbit [46] or human platelets [15] also develops at a slower rate, suggesting that this may be a trend of platelets' response to microbial ureases, contrasting to the much faster rate of Canatoxin- or JBU-induced effects [48]. Testing the subunits demonstrated that only PmUreβ induced aggregation of human platelets (Fig. 7B and C). PmUreγ did not interact at all with platelets. The maximal molar concentration of PmUreα that could be tested was 5.5-fold lower than that of PmUreβ, what may explain the lack of platelet aggregating effect. These results contrasts to the fact that both subunits of HPU interacted with human platelets [12], but only HpUreα (or B subunit), which is collinear to PmUreα, showed platelet-aggregating activity [12]. The sequence in HPU that corresponds to PmUreβ is part of its A subunit, where it appears fused to the sequence corresponding the PmUreγ (Fig. 9). A plausible explanation for this observation is that the region corresponding to PmUreγ poses some sort of steric hindrance that blocks a productive interaction of β domain in HPU's A subunit with platelets, thus abrogating an aggregation response. Nevertheless, HPU's A subunit produced other effects on platelets [15]. Altogether, these findings indicate that PMU is able to activate platelets (as do all other ureases we have tested so far) and this effect involves PmUreβ. Finally, the ability of ureases to insert themselves into lipid membranes, leading to formation of ion channels and to alterations of the membrane's permeability [49], could be what underlies their effects on different cell types.

The fact that PmUreβ displayed all the biological activities tested here was somewhat surprising. Apart from the catalytic region in the α subunit, no functions are yet clearly ascribed to the other bacterial enzyme's subunits. The urease's β domain has so far only been proposed to take part in the enzyme's activation process [72,73]. Since the biological effects of PmUreβ seen here overlapped the toxicity reported for Jaburetox, similarities between them were examined. Both, PmUreβ (this work) and Jaburetox [49] are located at the surface of the protein (Fig. 8), and therefore they could putatively "drive" many of the urease's interactions with other molecules and cells. Jaburetox is an intrinsically disordered peptide, a feature that may be at the basis of its toxicity [30,31,50]. Here, simulations of PmUreβ indicated loss of secondary structure that, accelerated under fold-disturbing conditions, yielded an unstructured molecule (Fig. 8). Thus, PmUreβ displays a Jaburetox-like behavior both in terms of biological activities and of physicochemical behavior. Although no obvious homology could be found by direct comparison of the amino acid sequences, a tool able to detect intragenic duplications on three levels revealed, in PmUreβ, a homologue of Jaburetox's sequence (Fig. 9A and C). Considering that, in contrast to Jaburetox, PmUreβ also activated platelets, additional regions of duplication between the β and α domains of JBU were inspected, revealing a second similarity site (Fig. 9A and C).

5. Conclusion

Considering the moonlighting profile of ureases' biological properties, here demonstrated also for PMU, we believe that the relevance of this protein as a virulence factor has been so far underappreciated. Its non-enzymatic properties suggest that PMU could probably be involved in many more features of *P. mirabilis* pathogenesis than merely providing nitrogen and shelter (by forming urinary stones) for the bacteria.

Ureases are unnecessarily large for the enzyme function they perform [38]. The need for the additional subunits (considering the ancestral dihydroorotase) is unknown, and acquisition of toxicity has been proposed as a trend [74]. Evidence of duplication within ureases genes have not been reported so far. Our current observation of duplications of "toxic" elements across urease subunits gives support to this proposition. Considering the evolutionary age of ureases and observing the conservation of a Jaburetox-like region in the β domain of the proteins may even point to its origin there, and the Jaburetox moiety in single-chained ureases could be labeled as a copy of an "original" toxic segment in the β subunit of tri-chained bacterial ureases (Fig. 6B). Confirmation that these enzymes may be accumulating various types of toxicities to become multifunctional toxins raises the question: was urease originally a toxin, then later co-opted for enzymatic activity [4]? While this question remains unanswered, PMU is clearly pointing towards toxicity as a driving force in the evolution of these enzymes.

Declaration of Competing Interest

The authors declare that they have no known competing financial interests or personal relationships that could have appeared to influence the work reported in this paper.

Acknowledgements

The authors thank Daniel Sulis for technical assistance and Dr. Barbara Zambelli (University of Bologna, Italy) for helping with plasmid construction of the *P. mirabilis* structural subunits. VB thanks Professor Stefano Ciurli for hosting her at the University of Bologna, Italy, and for the productive scientific support. This project was financed by the

Brazilian agencies CAPES - Coordenação de Aperfeiçoamento de Pessoal de Nível Superior (Finance code 001; Science Without Borders Program for Visiting Researcher – PVE 054/2012, and Edital Toxinologia – grant 63/2010); CNPq – Conselho Nacional de Desenvolvimento Científico e Tecnológico, Edital Universal, grants 44.6052/2014-1 and 47.5908/2012-0), and FAPERGS (Fundação de Amparo a Pesquisa do Estado do Rio Grande do Sul), Ed. PPSUS, grant 17/2551-0001451-0. VB received a split PhD fellowship (PVE 054/2012) from CAPES, for studies at the University of Bologna, Italy. LLF had a post-doctoral fellowship from the Young Talent Science Without Borders Program, CNPq grant 40.0189/2014-3. VB, FCL, MVCG, AHSM, AFU, RL-B were recipients of CAPES postgraduate fellowships.

Appendix A. Supplementary data

Supplementary material related to this article can be found, in the online version, at https://doi.org/10.1016/j.procbio.2021.08.023.

References

[1] K. Kappaun, A.R. Piovesan, C.R. Carlini, R. Ligabue-Braun, Ureases: historical aspects, catalytic and non-catalytic properties-a review, J. Adv. Res. (2018) 3–17.
[2] M.J. Maroney, S. Ciurli, Nonredox nickel enzymes, Chem. Rev. 114 (2014) 4206–4228.
[3] H.L. Mobley, R.P. Hausinger, Microbial ureases: significance, regulation, and molecular characterization, Microbiol. Rev. 53 (1989) 85–108.
[4] C.R. Carlini, R. Ligabue-Braun, Ureases as multifunctional toxic proteins: a review, Toxicon. 110 (2016) 90–109, https://doi.org/10.1016/j.toxicon.2015.11.020.
[5] B. Krajewska, I. Ureases, Functional, catalytic and kinetic properties: a review, J. Mol. Catal. B Enzym. 59 (2009) 9–21, https://doi.org/10.1016/j.molcatb.2009.01.003.
[6] P.A. Karplus, M.A. Pearson, R.P. Hausinger, 70 years of crystalline urease: what have we learned? Acc. Chem. Res. 30 (1997) 330–337.
[7] B. Zambelli, F. Musiani, S. Benini, S. Ciurli, Chemistry of Ni^{2+} in urease: sensing, trafficking, and catalysis, Acc. Chem. Res. 44 (2011) 520–530.
[8] F. Mulinari, F. Staniscuaski, L.R. Bertholdo-Vargas, M. Postal, O.B. Oliveira-Neto, D.J. Rigden, M.F. Grossi-de-Sá, C.R. Carlini, Jaburetox-2Ec: an insecticidal peptide derived from an isoform of urease from the plant Canavalia ensiformis, Peptides. 28 (2007) 2042–2050, https://doi.org/10.1016/j.peptides.2007.08.009.
[9] M. Postal, A.H.S. Martinelli, A.B. Becker-Ritt, R. Ligabue-Braun, D.R. Demartini, S. F.F. Ribeiro, G. Pasquali, V.M. Gomes, C.R. Carlini, Antifungal properties of *Canavalia ensiformis* urease and derived peptides, Peptides 38 (2012) 22–32, https://doi.org/10.1016/j.peptides.2012.08.010.
[10] K. Kappaun, A.H.S. Martinelli, V. Broll, B. Zambelli, F.C. Lopes, R. Ligabue-Braun, L.L. Fruttero, N.R. Moyetta, C.D. Bonan, C.R. Carlini, S. Ciurli, Soyuretox, an intrinsically disordered polypeptide derived from soybean (*Glycine max*) ubiquitous urease with potential use as a biopesticide, Int. J. Mol. Sci. 20 (2019) 1–20, https://doi.org/10.3390/ijms20215401.
[11] M.V.C. Grahl, F.C. Lopes, A.H.S. Martinelli, C.R. Carlini, L.L. Fruttero, Structure-function insights of Jaburetox and soyuretox: novel intrinsically disordered polypeptides derived from plant ureases, Molecules 25 (2020) 1–24, 5338.
[12] A.C. Costa, C. Figueiredo, E. Touati, Pathogenesis of Helicobacter pylori infection, Helicobacter 14 (2009) 15–20.
[13] J.-Y. Zhang, T. Liu, H. Guo, X.-F. Liu, Y. Zhuang, S. Yu, L. Chen, C. Wu, Z. Zhao, B. Tang, et al., Induction of a Th17 cell response by *Helicobacter pylori* Urease subunit B, Immunobiology 216 (2011) 803–810.
[14] J.H. Lee, S.H. Jun, J.-M. Kim, S.C. Baik, J.C. Lee, Morphological changes in human gastric epithelial cells induced by nuclear targeting of *Helicobacter pylori* urease subunit A, J. Microbiol. 53 (2015) 406–414.
[15] A. Scopel-Guerra, D. Olivera-Severo, F. Staniscuaski, A.F. Uberti, N. Callai-Silva, N. Jaeger, B.N. Porto, C.R. Carlini, The impact of *Helicobacter pylori* urease upon platelets and consequent contributions to inflammation, Front. Microbiol. 8 (2017) 1–13, 2447.
[16] C.E. Armbruster, H.L.T. Mobley, M.M. Pearson, Pathogenesis of *Proteus mirabilis* infection, EcoSal Plus 8 (2018) 1–123.
[17] H.L.T. Mobley, *Proteus mirabilis* overview. *Proteus Mirabilis*, Springer, 2019, pp. 1–4.
[18] B.D. Jones, C.V. Lockatell, D.E. Johnson, J.W. Warren, H.L. Mobley, Construction of a urease-negative mutant of *Proteus mirabilis*: analysis of virulence in a mouse model of ascending urinary tract infection, Infect. Immun. 58 (1990) 1120–1123.
[19] J.N. Schaffer, A.N. Norsworthy, T.-T. Sun, M.M. Pearson, *Proteus mirabilis* fimbriae- and urease-dependent clusters assemble in an extracellular niche to initiate bladder stone formation, Proc. Natl. Acad. Sci. 113 (2016) 4494–4499.
[20] T. Alelign, B. Petros, Kidney stone disease: an update on current concepts, Adv. Urol. (2018) (2018) 1–12.
[21] M. Miraula, S. Ciurli, B. Zambelli, Intrinsic disorder and metal binding in UreG proteins from *Archae* hyperthermophiles: GTPase enzymes involved in the activation of Ni (II) dependent urease, JBIC J. Biol. Inorg. Chem. 20 (2015) 739–755.
[22] M.V.C. Grahl, A.F. Uberti, V. Broll, P. Bacaicoa-Caruso, E.F. Meirelles, C.R. Carlini, *Proteus mirabilis* urease: unsuspected non-enzymatic properties relevant to pathogenicity, Int. J. Mol. Sci. 22 (2021) 1–17, 7205.
[23] L.T. Hu, P.A. Foxall, R. Russell, H.L. Mobley, Purification of recombinant *Helicobacter pylori* urease apoenzyme encoded by ureA and ureB, Infect. Immun. 60 (1992) 2657–2666.
[24] M.M. Bradford, A rapid and sensitive method for the quantitation of microgram quantities of protein utilizing the principle of protein-dye binding, Anal. Biochem. 72 (1976) 248–254, https://doi.org/10.1016/0003-2697(76)90527-3.
[25] U.K. Laemmli, Cleavage of structural proteins during the assembly of the head of bacteriophage T4, Nature 227 (1970) 680–685.
[26] M.W. Weatherburn, Phenol-hypochlorite reaction for determination of ammonia, Anal. Chem. 39 (1967) 971–974.
[27] V. Sharma, R. Chaudhary, J.M. Khurana, K. Muralidhar, In-gel detection of urease activity by nitroprusside–thiol reaction, Phytochem. Anal. An Int. J. Plant Chem. Biochem. Tech. 19 (2008) 99–103.
[28] L.L. Fruttero, N.R. Moyetta, A.F. Uberti, M.V.C. Grahl, F.C. Lopes, V. Broll, D. Feder, C.R. Carlini, Humoral and cellular immune responses induced by the urease-derived peptide Jaburetox in the model organism *Rhodnius prolixus*, Parasit. Vectors 9 (2016) 1–14, https://doi.org/10.1186/s13071-016-1710-3.
[29] S. Trentin, R. Brandt, K. Rigon, A. Gomes, M. Vanusa, M. Tereza, I. Jacob, R. Baumvol, A. José, Potential of medicinal plants from the Brazilian semi-arid region (Caatinga) against *Staphylococcus epidermidis* planktonic and biofilm lifestyles, J. Ethnopharmacol. 137 (2011) 327–335, https://doi.org/10.1016/j.jep.2011.05.030.
[30] A.H.S. Martinelli, K. Kappaun, R. Ligabue-Braun, M.S. Defferrari, A.R. Piovesan, F. Staniscuaski, D.R. Demartini, C.A. Dal Belo, C.G.M. Almeida, C. Follmer, H. Verli, C.R. Carlini, G. Pasquali, Structure-function studies on jaburetox, a recombinant insecticidal peptide derived from jack bean (*Canavalia ensiformis*) urease, Biochim. Biophys. Acta - Gen. Subj. 1840 (2014) 935–944, https://doi.org/10.1016/j.bbagen.2013.11.010.
[31] V. Broll, A.H.S. Martinelli, F.C. Lopes, L.L. Fruttero, B. Zambelli, E. Salladini, O. Dobrovolska, S. Ciurli, C.R. Carlini, Structural analysis of the interaction between Jaburetox, an intrinsically disordered protein, and membrane models, Colloids Surf. B Biointerfaces 159 (2017) 849–860, https://doi.org/10.1016/j.colsurfb.2017.08.053.
[32] G.L. Galvani, L.L. Fruttero, M.F. Coronel, S. Nowicki, D.R. Demartini, M. S. Defferrari, M. Postal, L.E. Canavoso, C.R. Carlini, B.P. Settembrini, Effect of the urease-derived peptide Jaburetox on the central nervous system of *Triatoma infestans* (Insecta : heteroptera), BBA - Gen. Subj. 1850 (2015) 255–262, https://doi.org/10.1016/j.bbagen.2014.11.008.
[33] N.J. Lane, R.A. Leslie, L.S. Swales, Insect peripheral nerves: accessibility of neurohaemal regions to lanthanum, J. Cell. Sci. 18 (1975) 179–197.
[34] E.W. Sayers, J. Beck, J.R. Brister, E.E. Bolton, K. Canese, D.C. Comeau, K. Funk, A. Ketter, S. Kim, A. Kimchi, et al., Database resources of the national center for biotechnology information, Nucleic Acids Res. 48 (2020) D9.
[35] F. Sievers, A. Wilm, D. Dineen, T.J. Gibson, K. Karplus, W. Li, R. Lopez, H. McWilliam, M. Remmert, J. Söding, et al., Fast, scalable generation of high-quality protein multiple sequence alignments using Clustal Omega, Mol. Syst. Biol. 7 (2011) 539.
[36] A.-L. Abraham, E.P.C. Rocha, J. Pothier, Swelfe: a detector of internal repeats in sequences and structures, Bioinformatics. 24 (2008) 1536–1537.
[37] S. Kumar, G. Stecher, M. Li, C. Knyaz, K. Tamura, MEGA X: molecular evolutionary genetics analysis across computing platforms, Mol. Biol. Evol. 35 (2018) 1547–1549.
[38] R. Ligabue-Braun, F.C. Andreis, H. Verli, C.R. Carlini, 3-to-1: unraveling structural transitions in ureases, Naturwissenschaften 100 (2013) 459–467, https://doi.org/10.1007/s00114-013-1045-2.
[39] N. Eswar, B. Webb, M.A. Marti-Renom, M.S. Madhusudhan, D. Eramian, M. Shen, U. Pieper, A. Sali, Comparative protein structure modeling using Modeller, Curr. Protoc. Bioinforma. (2006) 5–6.
[40] S. Benini, P. Kosikowska, M. Cianci, L. Mazzei, A.G. Vara, Ł. Berlicki, S. Ciurli, The crystal structure of *Sporosarcina pasteurii* urease in a complex with citrate provides new hints for inhibitor design, JBIC J. Biol. Inorg. Chem. 18 (2013) 391–399.
[41] B. Hess, C. Kutzner, D. Van Der Spoel, E. Lindahl, GROMACS 4: algorithms for highly efficient, load-balanced, and scalable molecular simulation, J. Chem. Theory Comput. 4 (2008) 435–447.
[42] G. Settanni, A.R. Fersht, High temperature unfolding simulations of the TRPZ1 peptide, Biophys. J. 94 (2008) 4444–4453.
[43] M.D. Island, H.L. Mobley, *Proteus mirabilis* urease: operon fusion and linker insertion analysis of ure gene organization, regulation, and function, J. Bacteriol. 177 (1995) 5653–5660.
[44] M.A. Kabir, M.A. Hussain, Z. Ahmad, *Candida albicans*: a model organism for studying fungal pathogens, Int. Sch. Res. Not. 2012 (2012) 1–15.
[45] M.S. Defferrari, D.H. Lee, C.L. Fernandes, I. Orchard, C.R. Carlini, A phospholipase A2 gene is linked to Jack bean urease toxicity in the Chagas' disease vector *Rhodnius prolixus*, Biochim. Biophys. Acta - Gen. Subj. 1840 (2014) 396–405, https://doi.org/10.1016/j.bbagen.2013.09.016.
[46] G.E. Wassermann, D. Olivera-Severo, A.F. Uberti, C.R. Carlini, *Helicobacter pylori* urease activates blood platelets through a lipoxygenase-mediated pathway, J. Cell. Mol. Med. 14 (2010) 2025–2034, https://doi.org/10.1111/j.1582-4934.2009.00901.x.
[47] C.R. Carlini, J.A. Guimarães, J.M. Ribeiro, Platelet release reaction and aggregation induced by canatoxin, a convulsant protein: evidence for the involvement of the platelet lipoxygenase pathway, Br. J. Pharmacol. 84 (1985) 551–560.

[48] C. Follmer, F.V. Pereira, N.P. Da Silveira, C.R. Carlini, Jack bean urease (EC 3.5.1.5) aggregation monitored by dynamic and static light scattering, Biophys. Chem. 111 (2004) 79–87, https://doi.org/10.1016/j.bpc.2004.03.009.
[49] A.R. Piovesan, A.H.S. Martinelli, R. Ligabue-braun, J. Schwartz, C.R. Carlini, *Canavalia ensiformis* urease, Jaburetox and derived peptides form ion channels in planar lipid bilayers, Arch. Biochem. Biophys. 547 (2014) 6–17, https://doi.org/10.1016/j.abb.2014.02.006.
[50] F.C. Lopes, O. Dobrovolska, R.R. Guerra, V. Broll, B. Zambelli, F. Musiani, V. N. Uversky, C.R. Carlini, S. Ciurli, Pliable natural biocide: jaburetox is an intrinsically disordered insecticidal and fungicidal polypeptide derived from jack bean urease, FEBS J. (2015) 1043–1064, https://doi.org/10.1111/febs.13201.
[51] C.F. Benjamin, C.R. Carlini, C. Barja-Fidalgo, Pharmacological characterization of rat paw edema induced by canatoxin, the toxic protein from *Canavalia ensiformis* (jack bean) seeds, Toxicon. 30 (1992) 879–885, https://doi.org/10.1016/0041-0101(92)90386-J.
[52] A.F. Uberti, D. Olivera-Severo, G.E. Wassermann, A. Scopel-Guerra, J.A. Moraes, P. Barcellos-de-Souza, C. Barja-Fidalgo, C.R. Carlini, Pro-inflammatory properties and neutrophil activation by *Helicobacter pylori* urease, Toxicon. 69 (2013) 240–249, https://doi.org/10.1016/j.toxicon.2013.02.009.
[53] A.E.A. Oliveira, V.M. Gomes, M.P. Sales, K.V.S. Fernandes, C.R. Carlini, J. Xavier-Filho, The toxicity of jack bean [*Canavalia ensiformis* (L.) DC.] canatoxin to plant pathogenic fungi, Rev. Bras. Biol. 59 (1999) 59–62, https://doi.org/10.1590/S0034-71081999000100008.
[54] A.B. Becker-Ritt, a.H.S. Martinelli, S. Mitidieri, V. Feder, G.E. Wassermann, L. Santi, M.H. Vainstein, J.T. a Oliveira, L.M. Fiuza, G. Pasquali, C.R. Carlini, Antifungal activity of plant and bacterial ureases, Toxicon. 50 (2007) 971–983, https://doi.org/10.1016/j.toxicon.2007.07.008.
[55] K.-H. Lee, S.J. Park, S.J. Choi, J.Y. Park, *Proteus vulgaris* and *Proteus mirabilis* decrease *Candida albicans* biofilm formation by suppressing morphological transition to its hyphal form, Yonsei Med. J. 58 (2017) 1135–1143.
[56] M.C. Furlaneto, C.G.T. de Jesus Andrade, L. Furlaneto-Maia, E.J.G. de França, A.T. P. Moralez, Pathogenic attributes of non-*Candida albicans* Candida species revealed by SEM. Scan. Electron Microsc., IntechOpen, 2012, pp. 295–310.
[57] H.-S. Lee, Y. Kim, *Aucklandia lappa* causes cell wall damage in *Candida albicans* by reducing chitin and (1, 3)-β-D-glucan, J. Microbiol. Biotechnol. 30 (2020) 967–973.
[58] J.D.M. Salvadori, M.S. Defferrari, R. Ligabue-Braun, E. Yamazaki Lau, J. R. Salvadori, C.R. Carlini, Characterization of entomopathogenic nematodes and symbiotic bacteria active against *Spodoptera frugiperda* (Lepidoptera: noctuidae) and contribution of bacterial urease to the insecticidal effect, Biol. Control 63 (2012) 253–263, https://doi.org/10.1016/j.biocontrol.2012.08.002.
[59] I. Chouikha, B.J. Hinnebusch, Silencing urease : A key evolutionary step that facilitated the adaptation of *Yersinia pestis* to the flea-borne transmission route, Proc. Natl. Acad. U. S. A 111 (2014) 18709–18714, https://doi.org/10.1073/pnas.1413209111.
[60] L.L. Fruttero, N.R. Moyetta, M.S. Krug, V. Broll, M.V.C. Grahl, R. Real-Guerra, F. Stanisçuaski, C.R. Carlini, Jaburetox affects gene expression and enzyme activities in *Rhodnius prolixus*, a Chagas' disease vector, Acta Trop. 168 (2017) 54–63.
[61] T. Carrazoni, M. de Avila Heberle, A.P.A. Perin, A.P. Zanatta, P.V. Rodrigues, F.D. M. dos Santos, C.G.M. de Almeida, R.V. Breda, D.S. dos Santos, P.M. Pinto, J. C. Costa, C.R. Carlini, C.A. Dal Belo, Central and peripheral neurotoxicity induced by the Jack Bean Urease (JBU) in *Nauphoeta cinerea* cockroaches, Toxicology. 368 (2016) 162–171.
[62] T. Carrazoni, C. Nguyen, L.F. Maciel, A. Delgado-Cañedo, B.A. Stewart, A.B. Lange, C.A. Dal Belo, C.R. Carlini, I. Orchard, Jack bean urease modulates neurotransmitter release at insect neuromuscular junctions, Pestic. Biochem. Physiol. 146 (2018) 63–70.
[63] D. Arendt, K. Nubler-Jung, Comparison of early nerve cord development in insects and vertebrates, Development 126 (1999) 2309–2325.
[64] W. Blenau, A. Baumann, Molecular and pharmacological properties of insect biogenic amine receptors: lessons from *Drosophila melanogaster* and *Apis mellifera*, Arch. Insect Biochem. Physiol. Publ. Collab. with Entomol. Soc. Am. 48 (2001) 13–38.
[65] C. Barja-Fidalgo, J.A. Guimarães, C.R. Carlini, Lipoxygenase-mediated secretory effect of canatoxin the toxic protein from *Canavalia ensiformis* seeds, Toxicon 29 (1991) 453–459, https://doi.org/10.1016/0041-0101(91)90019-N.
[66] S. Baik, H. Kang, J. Seo, E. Park, K. Rhee, M. Cho, *Helicobacter pylori* urease induces mouse death, J. Bacteriol. Virol. 35 (2005) 175–181.
[67] H. Phan, D. Lehman, Cerebral abscess complicating *Proteus mirabilis* meningitis in a newborn infant, J. Child Neurol. 27 (2012) 405–407.
[68] I.S. Kourbeti, A.F. Vakis, P. Ziakas, D. Karabetsos, E. Potolidis, S. Christou, G. Samonis, Infections in patients undergoing craniotomy: risk factors associated with post-craniotomy meningitis, J. Neurosurg. 122 (2015) 1113–1119.
[69] C.-H. Lu, W.-N. Chang, C.-C. Lui, P.-Y. Lee, H.-W. Chang, Adult spinal epidural abscess: clinical features and prognostic factors, Clin. Neurol. Neurosurg. 104 (2002) 306–310.
[70] N. Browne, M. Heelan, K. Kavanagh, An analysis of the structural and functional similarities of insect hemocytes and mammalian phagocytes, Virulence 4 (2013) 597–603.
[71] T. Zielinski, B. Wachowicz, J. Saluk-Juszczak, W. Kaca, Polysaccharide part of *Proteus mirabilis* lipopolysaccharide may be responsible for the stimulation of platelet adhesion to collagen, Platelets 13 (2002) 419–424.
[72] F. Musiani, D. Gioia, M. Masetti, F. Falchi, A. Cavalli, M. Recanatini, S. Ciurli, Protein tunnels: the case of urease accessory proteins, J. Chem. Theory Comput. 13 (2017) 2322–2331.
[73] S. Quiroz-Valenzuela, S.C.K. Sukuru, R.P. Hausinger, L.A. Kuhn, W.T. Heller, The structure of urease activation complexes examined by flexibility analysis, mutagenesis, and small-angle X-ray scattering, Arch. Biochem. Biophys. 480 (2008) 51–57.
[74] R. Ligabue-Braun, C.R. Carlini, Moonlighting toxins: ureases and beyond. Plant Toxins, Springer, 2015, pp. 1–21.